Spectrochimica Acta Part A: Molecular and Biomolecular Spectroscopy 129 (2014) 7–13

Contents lists available at ScienceDirect

Spectrochimica Acta Part A: Molecular and Biomolecular Spectroscopy

journal homepage: www.elsevier.com/locate/saa

Synthesis of quinoline derivatives containing pyrazole group and investigation of their crystal structure and spectroscopic properties in relation to acidity and alkalinity of mediums

Tiegang Ren [a], Jie Wang [a], Guihui Li [b,*], Hongbin Cheng [a], Yongzhe Li [a]

[a] Fine Chemistry and Engineering Research Institute, College of Chemistry and Chemical Engineering, Henan University, Kaifeng 475004, People's Republic of China
[b] Key Laboratory of Ministry of Education for Special Functional Materials, Henan University, Kaifeng 475004, People's Republic of China

HIGHLIGHTS

- A series of quinoline derivatives containing pyrazole group were synthesized and characterized.
- The UV–vis spectra and fluorescent spectra of various as-synthesized products were measured.
- The effect of acetic acid and triethylamine on the spectroscopic properties of as-synthesized products was examined.

GRAPHICAL ABSTRACT

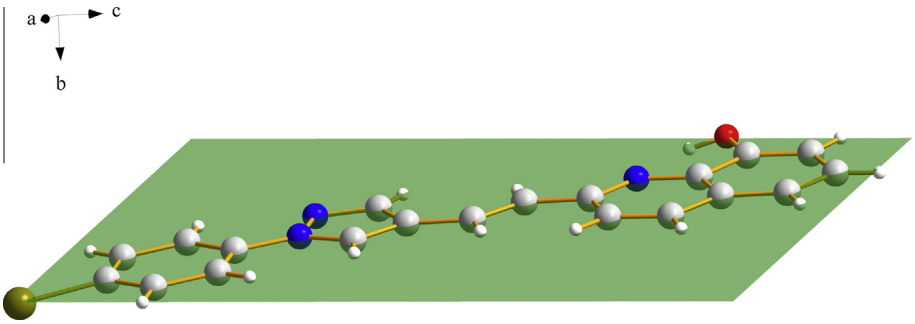

ARTICLE INFO

Article history:
Received 22 January 2014
Received in revised form 12 March 2014
Accepted 15 March 2014
Available online 22 March 2014

Keywords:
Quinoline derivative
Pyrazole group
Synthesis
Acidity and alkalinity of medium
Spectroscopic properties
Theoretical investigations

ABSTRACT

Two series of quinoline derivatives containing pyrazole group were synthesized and characterized by means of ^{1}H NMR, FT-IR, MS, elemental analysis and X-ray single crystal diffraction, and their UV–vis absorption behavior and fluorescence properties were also measured. Moreover, the effects of acetic acid and triethylamine on the spectroscopic properties of synthesized products were examined with compounds **3a** and **5a** as examples. It has been found that all synthesized quinoline derivatives show maximum absorption peak at 303 nm and emission peaks around 445 nm. Besides, both acetic acid and triethylamine can change the acidity of the medium, thereby influencing the UV–vis absorption spectra and fluorescence spectra of synthesized products. Moreover, theoretical investigations indicate that the integration of H^+ and N atom of quinoline ring favors the formation of a new product in the presence of acetic acid, and the product obtained in this case shows a new UV–vis absorption peak at 400 nm.

Introduction

As a class of important heterocyclic compounds, quinoline compounds display a wide range of applications and development prospects in healthcare, ion recognition, fluorescent probe and optical functionalization [1]. Particularly, 8-hydroxyquinoline derivatives are significant intermediates in pharmaceutical industry [2], because as a kind of integrase inhibitors they can effectively inhibit HIV-1s [3], impede retroviral integrase [4], prevent protozoa and retroviral mixed infection [5], and eliminate free radicals and inhibit lipid peroxidation [6]. Furthermore, 8-hydroxyquinoline derivatives can also be applied as organic photoelectric functional materials. For example, in 1987, Tang et al. reported a green emitting device prepared from 8-hydroxyquinoline aluminum as the light emitting layer [7]. Since then, many quinoline

* Corresponding author. Tel.: +86 378 2866141.
E-mail address: rtg@henu.edu.cn (G. Li).

http://dx.doi.org/10.1016/j.saa.2014.03.018
1386-1425/

compounds have been designed, synthesized and used as photoelectric functional materials. In the meantime, as an important family of organic fluorescent compounds, pyrazole derivatives are useful reagents for the extraction and separation of various metal ions [8,9], and they are also of significance in anti-virus, anticancer, anti-fungus, anti-inflammatory, and anti-oxidation as well as for treatment of hypoglycemia and physiological disorders [10,11]. This reminds us that, by integrating quinoline with pyrazole group, it may be feasible to synthesize novel quinoline derivatives as multifunctional pharmaceutical intermediates or even drugs.

In our previous work, we synthesized a series of Schiff base compounds and benzimidazole compounds containing pyrazole group, and found that the introduction of pyrazole group to the molecular chain of Schiff base or benzimidazole compounds led to enhanced fluorescence emissions [12–14]. Unfortunately, little is currently available about the fluorescent properties of quinoline derivatives containing pyrazole group and about the correlation between their molecular structure and emission properties, which greatly hinders their applications in biological and environmental sciences. Thus in this article we report a simple procedure for synthesizing quinoline derivatives containing pyrazole group as well as their molecular and crystal structures and fluorescent properties.

Experiments

Physical measurement and materials

Mass spectra (MS) were determined with an Agilent 1100LC-MS mass spectrometer. Infrared (IR) spectra of obtained products within 400–4000 cm^{-1} were recorded with a Nicolet 170 SXFT-IR spectrometer (mixed with KBr and pressed into pellets). Nuclear magnetic resonance (^{1}H NMR) spectra in $(CD_3)_2CO$ solvent were recorded with an INOVA-400 spectrometer in the presence of tetramethylsilane as an internal standard. Elemental analysis was conducted with a PE2400 elemental analysis apparatus. Ultraviolet–visible light (UV–vis) absorption spectra of target compounds in a wavelength range of 200–700 nm were measured with a Hitachi U-4100 spectrophotometer (to-be-tested compounds were separately dissolved in spectral grade dimethylfomamide (DMF) at a concentration of 1.0×10^{-5} mol/L). The fluorescence spectra of various target compounds separately dissolved in spectral grade DMF at a concentration of 1.0×10^{-5} mol/L were recorded with a Hitachi F-7000 spectrofluorometer in right angle detection mode (each solution was excited at λ_{max} and the corrected fluorescence emission spectrum was recorded also at a wavelength of 200–700 nm). Specifically, target compounds **3a** and **5a** were separately dissolved in spectral grade DMF at a concentration of 1.0×10^{-5} mol/L while the concentration of acetic acid or triethylamine was adjusted within 3.0×10^{-5}–1.75×10^{-3} mol/L so as to explore the influence of acidity and alkalinity of the medium on the spectroscopic properties of target products.

All chemicals and solvents are of commercial reagent grade and used without further purification. 1-Arylpyrazole-4-carbaldehyde was prepared according to procedures available elsewhere [15]. Known structures of 1-arylpyrazole-4-carbaldehyde were verified by comparing their data with those reported in the literature [13–15].

General procedure for preparing (E)-2-(2-(1-aryl-1H-pyrazol-4-yl) vinyl)quinolin-8-ol

5 mmol 1-Arylpyrazole-4-carbaldehyde, 5 mmol 2-methyl-8-hydroxyl quinoline and 20 mL acetic anhydride were stirred and sealed in a Teflon-lined stainless steel autoclave (25 mL), kept at 160 °C for 4 days and then cooled to room temperature. Resultant mixed solution was poured into 100 mL H_2O, followed by extraction with CH_2Cl_2 (3×50 mL) and rotary evaporation to remove solvent. As-separated crystalline precipitates were dissolved in 25 mL DMF, followed by dropwise addition of 20 mL of aqueous HCl (volume fraction: 36%) at 80 °C in a reaction period of 5 h. Then the reactants were allowed to react for additional 4 h after 25 mL of triethylamine was added dropwise. Upon completion of the reaction, the hot mixture was poured into ice water (250 mL) and stirred overnight, followed by extraction with CH_2Cl_2 (4×100 mL). The combined organic layers were washed with saturated NaCl solution and dried with anhydrous Na_2SO_4. Crude mixed products were obtained after residual solvent was evaporated under reduced pressure, and as-obtained crude products were purified by column chromatography (silica gel, ethyl acetate/petroleum ether).

(*E*)-2-(2-(1-(3,4-dimethylphenyl)-3,5-dimethyl-1H-pyrazol-4-yl)vinyl)quinolin-8-ol (**1a**), pale-yellow solid 0.94 g, yield 50.8%. Electrospray ionization mass spectra (ESI-MS, *m*/*z*): 370.20(M^+). ^{1}H NMR ($(CD_3)_2CO$) δ: 2.31 (s, 3H, CH_3), 2.33 (s, 3H, CH_3), 2.48 (s, 3H, CH_3), 2.50 (s, 3H, CH_3), 2.89 (s, 1H, O—H), 7.08–7.13 (m, 2H, quinolin-H), 7.22–7.40 (m, 5H, quinolin-H, Ar—H), 7.77–7.79 (d, J = 8.0 Hz, 1H, quinolin-H), 7.99–8.01 (d, J = 8.0 Hz, 1H, C=C—H), 8.23–8.25 (d, J = 8.0 Hz, 1H, C=C—H). IR (KBr, cm^{-1}) ν: 3370.87, 1642.72, 1456.31, 1145.63, 951.46. Anal. Calc.: C, 78.02; H, 6.27; N, 11.37. Found: C, 77.85; H, 6.09; N, 11.27.

(*E*)-2-(2-(3,5-dimethyl-1-(p-tolyl)-1H-pyrazol-4-yl)vinyl)quinolin-8-ol (**2a**), pale-yellow solid 0.88 g, yield 49.4%. ESI-MS (*m*/*z*): 356.20(M^+). ^{1}H NMR ($(CD_3)_2CO$) δ: 2.39 (s, 3H, CH_3), 2.48 (d, J = 4.0 Hz, 6H, CH_3), 3.37 (s, 1H, O—H), 7.07–7.13 (m, 2H, quinolin-H), 7.33–7.41 (m, 6H, quinolin-H, Ar—H), 7.78–7.80 (d, J = 8.0 Hz, 1H, quinolin-H), 7.97–7.99 (d, J = 8.0 Hz, 1H, C=C—H), 8.23–8.25 (d, J = 8.0 Hz, 1H, C=C—H). IR (KBr, cm^{-1}) ν: 3340.12, 1638.83, 1456.31, 1145.63, 955.34. Anal. Calc.: C, 77.72; H, 5.96; N, 11.82. Found: C, 77.69; H, 6.10; N, 11.68.

(*E*)-2-(2-(3,5-dimethyl-1-phenyl-1H-pyrazol-4-yl)vinyl)quinolin-8-ol (**3a**), pale-yellow solid 0.89 g, yield 52.0%. ESI-MS (*m*/*z*): 342.20(M^+). ^{1}H NMR ($(CD_3)_2CO$) δ: 2.39 (s, 3H, CH_3), 2.52 (s, 3H, CH_3), 3.37 (s, 1H, O—H), 7.07–7.14 (m, 2H, quinolin-H), 7.34–7.45 (m, 3H, Ar—H), 7.52–7.57 (m, 4H, quinolin-H, Ar—H), 7.79–7.81 (d, J = 8.0 Hz, 1H, quinolin-H), 7.98–8.00 (d, J = 8.0 Hz, 1H, C=C—H), 8.23–8.25 (d, J = 8.0 Hz, 1H, C=C—H). IR (KBr, cm^{-1}) ν: 3389.03, 1634.95, 1429.13, 1130.10, 955.34. Anal. Calc.: C, 77.40; H, 5.61; N, 12.31. Found: C, 77.24; H, 5.41; N, 12.19.

(*E*)-2-(2-(1-(4-fluorophenyl)-3,5-dimethyl-1H-pyrazol-4-yl)vinyl)quinolin-8-ol (**4a**), pale-yellow solid 0.77 g, yield 42.7%. ESI-MS (*m*/*z*): 360.2(M^+). 1H NMR ($(CD_3)_2CO$) δ: 2.48 (s, 3H, CH_3), 2.49 (s, 3H, CH_3), 3.36 (s, 1H, O—H), 7.07–7.13 (m, 2H, quinolin-H), 7.28–7.40 (m, 4H, Ar—H), 7.55–7.59 (m, 2H, quinolin-H), 7.78–7.80 (d, J = 8.0 Hz, 1H, quinolin-H), 7.96–7.98 (d, J = 8.0 Hz, 1H, C=C—H), 8.22–8.24 (d, J = 8.0 Hz, 1H, C=C—H). IR (KBr, cm^{-1}) ν: 3356.82, 1642.84, 1455.22, 1155.28, 960.14. Anal. Calc.: C, 73.52; H, 5.05; N, 11.69. Found: C, 73.36; H, 4.84; N, 11.53.

(*E*)-2-(2-(1-(4-chlorophenyl)-3,5-dimethyl-1H-pyrazol-4-yl)vinyl)quinolin-8-ol (**5a**), pale-yellow solid 0.87 g, yield 46.0%. ESI-MS (*m*/*z*): 376.20(M^+). ^{1}H NMR ($(CD_3)_2CO$) δ: 2.49 (s, 3H, CH_3), 2.53 (s, 3H, CH_3), 3.34 (s, 1H, O-H), 7.07–7.14 (m, 2H, quinolin-H), 7.34–7.40 (m, 2H, quinolin-H), 7.55–7.58 (m, 4H, Ar—H), 7.78–7.80 (d, J = 8.0 Hz, 1H, quinolin-H), 7.96–7.98 (d, J = 8.0 Hz, 1H, C=C—H), 8.23–8.25 (d, J = 8.0 Hz, 1H, C=C—H). IR(KBr, cm^{-1}) ν: 3345.31, 1642.95, 1145.38, 959.22. Anal. Calc.: C, 70.30; H, 4.83; N, 11.18. Found: C, 70.08; H, 4.45; N, 10.95.

(*E*)-2-(2-(1-(4-bromophenyl)-3,5-dimethyl-1H-pyrazol-4-yl)vinyl)quinolin-8-ol (**6a**), pale-yellow solid 0.96 g, yield 45.7%. ESI-MS (*m*/*z*): 422.10(M^+). ^{1}H NMR ($(CD_3)_2CO$) δ: 2.50 (s, 3H, CH_3), 2.56 (s, 3H, CH_3), 2.87 (s, 1H, O—H), 7.08–7.16 (m, 2H, quinolin-H), 7.34–7.42 (m, 2H, quinolin-H), 7.52–7.56 (m, 2H, Ar—H), 7.71–7.74

(m, 2H, Ar—H), 7.78–7.80 (d, J = 8.0 Hz, 1H, quinolin-H), 8.00–8.02 (d, J = 8.0 Hz, 1H, C=C—H), 8.24–8.26 (d, J = 8.0 Hz, 1H, C=C—H). IR (KBr, cm^{-1}) v: 3366.92, 1642.70, 1454.74, 1145.63, 955.34. Anal. Calc.: C, 62.87; H, 4.32; N, 10.00. Found: C, 63.05; H, 3.75; N, 9.86.

(*E*)-2-(2-(1-(3,4-dimethylphenyl)-1H-pyrazol-4-yl)vinyl)quinolin-8-ol (**1b**), pale-yellow solid 0.91 g, yield 53.2%. ESI-MS (m/z): 342.20(M^+). ^{1}H NMR ($(CD_3)_2CO$) δ: 2.29 (s, 3H, CH_3), 2.34 (s, 3H, CH_3), 2.87 (s, 1H, O—H), 7.10–7.12 (d, J = 8.0 Hz, 1H, quinolin-H), 7.25–7.42 (m, 4H, quinolin-H, Ar—H), 7.57–7.59 (m, 1H, quinolin-H), 7.67–7.71 (m, 2H, quinolin-H), 7.96–7.98 (d, J = 8.0 Hz, 1H, C=C—H), 8.05 (s, 1H, pyrazol-H), 8.24–8.26 (d, J = 8.0 Hz, 1H, C=C—H), 8.58 (s, 1H, pyrazol-H). IR (KBr, cm^{-1}) v: 3377, 1640, 1459, 1164, 966. Anal. Calc.: C, 77.40; H, 5.61; N, 12.31. Found: C, 61.83; H, 3.73; N, 6.20.

(*E*)-2-(2-(1-(p-tolyl)-1H-pyrazol-4-yl)vinyl)quinolin-8-ol (**2b**), pale-yellow solid 1.01 g, yield 61.6%. ESI-MS (m/z): 328.20(M^+). ^{1}H NMR ($(CD_3)_2CO$) δ: 2.35 (s, 3H, CH_3), 3.38 (s, 1H, O—H), 7.08–7.11 (dd, J = 4.0 Hz, J = 8.0 Hz, 1H, quinolin-H), 7.29–7.41 (m, 5H, quinolin-H, Ar—H), 7.70–7.76 (m, 3H, Ar—H), 7.94–7.96 (d, J = 8.0 Hz, 1H, C=C—H), 8.08 (s, 1H, pyrazol-H), 8.24–8.26 (d, J = 8.0 Hz, 1H, C=C—H), 8.61 (s, 1H, pyrazol-H). IR (KBr, cm^{-1}) v: 3370.33, 1636.97, 1458.10, 1153.40, 950.87. Anal. Calc.: C, 77.04; H, 5.23; N, 12.84. Found: C, 76.93; H, 5.02; N, 12.74.

(*E*)-2-(2-(1-phenyl-1H-pyrazol-4-yl)vinyl)quinolin-8-ol (**3b**), pale-yellow solid 0.94 g, yield 59.9%. ESI-MS (m/z): 314.10(M^+). ^{1}H NMR ($(CD_3)_2CO$) δ: 3.34 (s, 1H, O—H), 7.55–7.57 (dd, J = 4.0 Hz, 1H, quinolin-H), 7.76–7.86 (m, 4H, quinolin-H, Ar—H), 7.97–8.01 (t, J = 8.0 Hz, 2H, Ar—H), 8.15–8.17 (d, J = 4.0 Hz, 1H, quinolin-H), 8.35–8.37 (d, J = 4.0 Hz, 2H, quinolin-H), 8.44–8.46 (d, J = 8.0 Hz, 1H, C=C—H), 8.56 (s, 1H, pyrazol-H), 8.71–8.73 (d, J = 8.0 Hz, 1H, C=C—H), 9.11 (s, 1H, pyrazol-H). IR (KBr, cm^{-1}) v: 3392.31, 1641.23, 1459.74, 1194.47, 951.70. Anal. Calc.: C, 76.66; H, 4.82; N, 13.41. Found: C, 70.00; H, 4.47; N, 13.20.

(*E*)-2-(2-(1-(4-fluorophenyl)-1H-pyrazol-4-yl)vinyl)quinolin-8-ol (**4b**), pale-yellow solid 0.89 g, yield 53.6%. ESI-MS (m/z): 332.20(M^+). ^{1}H NMR ($(CD_3)_2CO$) δ: 3.37 (s, 1H, O—H), 7.09–7.11 (m, 1H, quinolin-H), 7.28–7.41 (m, 5H, quinolin-H, Ar—H), 7.70–7.72 (d, J = 8.0 Hz, 1H, C=C—H), 7.89–7.98 (m, 3H, quinolin-H), 8.10 (s, 1H, pyrazol-H), 8.25–8.27 (d, J = 8.0 Hz, 1H, C=C—H), 8.64 (s, 1H, pyrazol-H). IR (KBr, cm^{-1}) v: 3404.48, 1641.78, 1459.78, 1154.20, 952.22. Anal. Calc.: C, 72.50; H, 4.26; N, 12.68. Found: C, 72.30; H, 3.90; N, 12.46.

(*E*)-2-(2-(1-(4-chlorophenyl)-1H-pyrazol-4-yl)vinyl)quinolin-8-ol (**5b**), pale-yellow solid 0.97 g, yield 55.9%. ESI-MS (m/z): 348.10(M^+). ^{1}H NMR ($(CD_3)_2CO$) δ: 7.10–7.12 (dd, J = 4.0 Hz, 1H, quinolin-H), 7.30–7.43 (m, 3H, quinolin-H, Ar—H), 7.53–7.57 (m, 2H, Ar—H), 7.89–7.93 (d, J = 4.0 Hz, 1H, quinolin-H), 7.89–7.95 (m, 2H, quinolin-H), 7.95–7.99 (d, J = 8.0 Hz, 1H, C=C—H), 8.12 (s, 1H, pyrazol-H), 8.25–8.27 (d, J = 8.0 Hz, 1H, C=C—H), 8.65 (s, 1H, pyrazol-H). IR (KBr, cm^{-1}) v: 3341.49, 1640.91, 1459.45, 1192.34, 947.59. Anal. Calc.: C, 69.07; H, 4.06; N, 12.08. Found: C, 69.06; H, 3.60; N, 11.88.

(*E*)-2-(2-(1-(4-bromophenyl)-1H-pyrazol-4-yl)vinyl)quinolin-8-ol (**6b**), pale-yellow solid 1.04 g, yield 53.2%. ESI-MS (m/z): 393.1(M^+). ^{1}H NMR ($(CD_3)_2CO$) δ: 2.89 (s, 1H, O—H), 7.09–7.11 (dd, J = 4.0 Hz, 1H, quinolin-H), 7.31–7.43 (m, 3H, quinolin-H, Ar—H), 7.69–7.71 (m, 3H, quinolin-H, Ar—H), 7.85–7.89 (m, 2H, quinolin-H), 7.98–8.00 (d, J = 8.0 Hz, 1H, C=C—H), 8.12 (s, 1H, pyrazol-H), 8.26–8.28 (d, J = 8.0 Hz, 1H, C=C—H), 8.67 (s, 1H, pyrazol-H). IR (KBr, cm^{-1}) v: 3340.85, 1639.24, 1458.92, 1192.22, 947.04. Anal. Calc.: C, 61.24; H, 3.60; N, 10.71. Found: C, 61.69; H, 2.92; N, 10.58.

Single crystal X-ray crystallography

Synthesized products **1a** and **6b** were used as typical examples for single crystal crystallographic analysis, where single crystal specimens **1a** (0.45 mm × 0.39 mm × 0.11 mm) and **6b** (0.43 mm × 0.35 mm × 0.26 mm) were acquired *via* slow evaporation of their ethanol solutions at room temperature. The reflection data were collected at 296(2) K in an $\omega/2\theta$ scan mode with graphite monochromated Mo Kα radiation (λ = 0.071073 nm) as the excitation source. The reflections of single crystal **1a** were measured in a 2θ range of 1.96–25.00°, and those of single crystal **6b** were measured in a 2θ range of 2.26–17.97°; and 2421 and 3812 independent reflections were measured for **1a** and **6b**, respectively. SADABS multi-scan empirical absorption corrections were adopted for data processing. The crystal structure was solved by direct method and refined based on full-matrix least-squares on F_2. The final least square cycle of refinement for **1a** gave R = 0.0465 and wR_2 = 0.1244; and that for **6b** gave R = 0.0879 and wR_2 = 0.1385.

Results and discussion

Synthesis

The synthetic route of 2-(2-(1-aryl-1H-pyrazol-4-yl)vinyl)quinolin-8-ol is outlined in Fig. 1.

2-(2-(1-Aryl-1H-pyrazol-4-yl)vinyl)quinolin-8-ol was synthesized by Perkin reaction with 2-methyl-8-hydroxy quinoline and 1-arylpyrazol-4-carbaldehyde as the starting materials. In the presence of acetic anhydride as the solvent, the 4 days reaction under 160 °C initially yields an acetate derivative. The acetoxyl group of the acetate derivative is hydrolyzed in the presence of hydrochloric acid to yield hydrochloric salt which is treated with triethylamine to afford desired target compound. Since the substrate of aryl aldehydes and the solvent (acetic anhydride) react to form carbonyl acetal ester, it is imperative to protect the carbonyl while aryl aldehyde is consumed to decrease the yield of the condensation reaction. Findings show that acidic medium favors the formation of carbonyl acetal ester but inhibits the formation of desired condensation product. Specially, substituent -CH_3 on the pyrazole group leads to decrease in the yield of target products (**a**-series), which might be due to larger steric hindrance of -CH_3 than that of H atom. Coupling constants of the hydrogen in the vinyl group of various target compounds suggest that they are of *trans*-conformation, which can be further confirmed by the IR spectrum and single crystal structure of compounds **1a** and **6b** as typical examples.

Crystallography and characterization

The crystallographic data, selected bond lengths and bond angles for target compounds **1a** and **6b** are listed in Tables s1–s3, respectively. The molecular structures of **1a** and **6b** are shown in Fig. 2. The N—C distances of compound **1a** (1.330(2) Å of N(1)—C(9), 1.368(2) Å of N(1)—C(1), and 1.426(2) Å of N(3)—C(17)) lie between those of typical double bond C=N (1.287 Å) and single bond C—N (1.471 Å); the O(1)—C(2) distance, 1.359(2) Å, is shorter than typical single bond C—O (1.43 Å) and indicates the formation of p–π conjugated systems; and the distances of C(9)—C(10) (1.461(2) Å) and C(11)—C(12) (1.448(2) Å) are shorter than typical single bond C—C (1.54 Å), due to the formation of conjugated systems. The bond lengths of compound **6b** are similar to those of compound **1a** (see Table s3). Particularly, the C(10)—C(11) (1.325(2) Å) of **1a** and C(10)—C(11) (1.298(6) Å) of **6b** are shorter than typical double bond C=C (1.34 Å). In the meantime, there are no intermolecular hydrogen bonds but only intramolecular hydrogen bonds in the tautomers of **1a** (see Fig. s1, Table s2) and **6b** (see Fig. s2, Table s3). The distances of the hydrogen bonds (O(1)—H(1)...N(1)) of compounds **1a** and **6b** are 2.6614(19) Å and 2.690(4) Å, respectively.

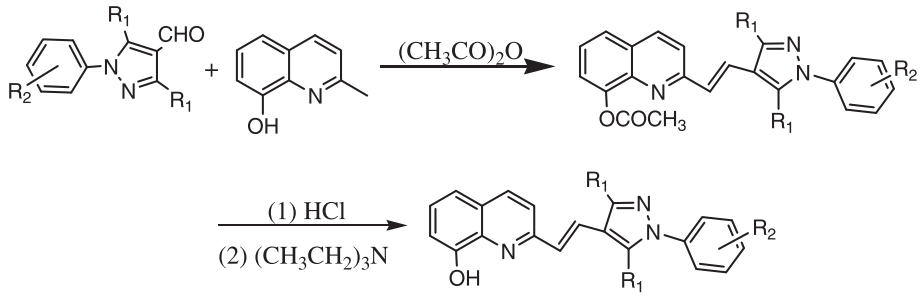

R_1=-CH_3 ; R_2=3,4-di-CH_3(**1a**); 4-CH_3(**2a**); -H(**3a**); 4-F(**4a**); 4-Cl(**5a**); 4-Br(**6a**)
R_1=H ; R_2=3,4-di-CH_3(**1b**); 4-CH_3(**2b**); -H(**3b**); 4-F(**4b**); 4-Cl(**5b**); 4-Br(**6b**)

Fig. 1. The synthetic route of 2-(2-(1-aryl-1H-pyrazol-4-yl)vinyl)quinolin-8-ol.

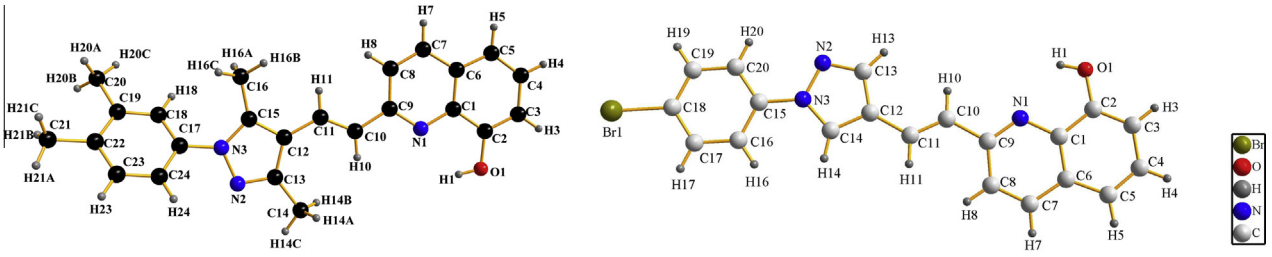

Fig. 2. Structure of compounds **1a** and **6b**.

Compound **6b** has planar molecular structure, and all of the atoms in **6b** molecule are located on the same plane, which is favorable for decreasing the energy levels of the molecule (Fig. s3). However, due to the existence of —CH_3, the atoms (except H in —CH_3) in **1a** molecule are located in two planes, and the dihedral angle is 35.3° (Fig. s4).

UV–vis spectra

Figs. 3 and 4 show the UV–vis spectra of the two series of target compounds. It can be seen that compounds **1a**–**6a** show three absorption peaks while compounds **1b**–**6b** show two absorption peaks. Namely, compounds **1a**–**6a** and compounds **1b**–**6b** show the same maximum absorption peak at 302–304 nm and the second absorption peak at 340–344 nm. Compounds **1a**–**6a** show

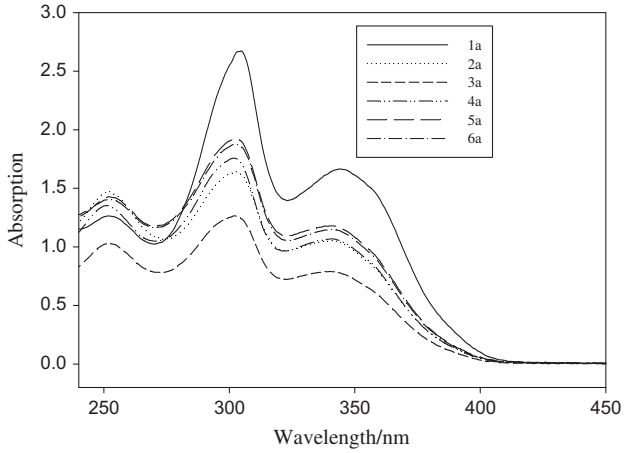

Fig. 3. UV–vis spectra of compounds **1a**–**6a**.

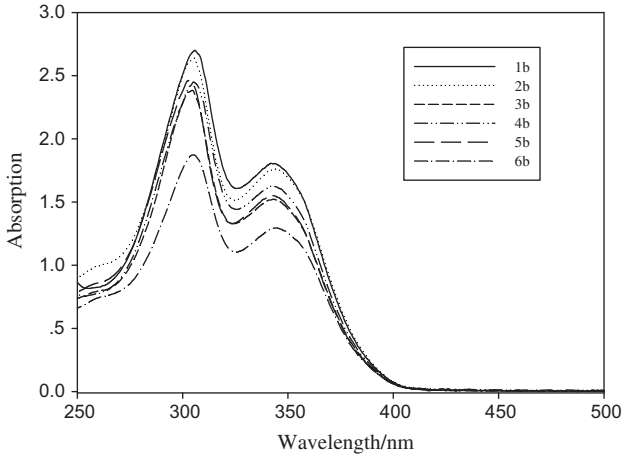

Fig. 4. UV–vis spectra of compounds **1b**–**6b**.

the third absorption peak at 252 nm, but compounds **1b**–**6b** do not show this absorption peak. The reason may lie in that compounds **1a**–**6a** contain two methyl groups connected with pyrazole ring, and the introduction of the alkyl group to the conjugated systems allows the electron of alkyl C—H bond to overlap with the π electron of the conjugated system (the so-called hyperconjugation). In the meantime, substituent *R* of the phenyl group connected with pyrazole ring also influences the absorption wavelength and absorbance. Namely, alkyl groups such as —CH_3 and 3,4-di-CH_3 lead to shift of the absorption peak towards longer wavelength, and the introduction of auxochrome groups such as —F, —Cl and —Br to the phenyl group allows conjugation of nonbonded electron with π electron to form p–π conjugation thereby leading to enhanced electronic scope of operation and shift of absorption peak towards longer wavelength.

Fluorescence spectra

The fluorescence spectra of the two series of target compounds are shown in Figs. 5 and 6. It can be seen that the two series of target compounds show an emission peak at 440–448 nm when their DMF solutions are excited at 290 nm (**a** series of products) or 275 nm (**b** series of products). Obviously, the shape and position of the emission peaks of the two series of target compounds are similar. However, the fluorescence intensity of **b** series of products is much higher than that of **a** series of products, which may be attributed to the planar molecular structure of **b** series of products. Moreover, the substituent R_2 of the phenyl group has a minor influence on the emission peak position and fluorescence intensity of target compounds, which may be a compromise between the electronic effect and space effect of the substituent.

*Influence of acidity or alkalinity of mediums on spectral properties of compounds **3a** and **5a***

Pyrazole as a twisted intramolecular charge transfer compound possesses structural units of electron donor-electron acceptor. Therefore, their intramolecular charge distribution as well as their spectral properties is closely related to the acidity or alkalinity of mediums. In the meantime, hydroxyquinoline compounds containing different active groups are able to form a variety of possible new compounds in acid and alkaline medium conditions (Fig. 7) thereby affecting the optical performance. For this reason, we choose compounds **3a** and **5a** as examples to explore the influence of the acidity or alkalinity of mediums on their spectral properties and to investigate the possible reaction mechanisms based on calculations of density functional theory (DFT) and time-dependent density functional theory (TD–DFT).

*Influence of acidity or alkalinity of mediums on UV–vis spectra of compounds **3a** and **5a***

The effect of acetic acid on the UV–vis spectra of compounds **3a** and **5a** is shown in Figs. 8 and 9. It can be seen that acetic acid leads to red-shifts of absorption peaks and form three new absorption peaks. In the meantime, with increasing concentration of acetic acid, the intensity of the absorption peak near 400 nm obviously rises but that of the peaks near 263 nm and 320 nm varies slightly. This suggests that new species are generated upon contact of compounds **3a** and **5a** with acetic acid *via* possible pathways shown in Fig. 7. To identify relevant products, we adopt DFT and TD–DFT to optimize their full geometries with B3LYP and M06 methods [16–18]. The UV–vis absorption spectra of compounds **3a** and **5a** in acetic acid are also simulated with PCM model of TD–DFT. Theoretical calculations indicate that the new species are formed *via* hydrogenation path (path b in Fig. 7). The theoretical spectrum of the hydrogenation product **3a**, (*E*)-2-(2-(3,5-dimethyl-1-phenyl-1*H*-pyrazol-4-yl)vinyl)-8-hydroxyquinolinium, covers three absorption peaks located at 273.12 (f = 0.1423), 317.29 (f = 0.3472), and 411.70 nm (f = 1.2393). Considering the solvent effect and experimental error, we can reasonably infer that the theoretically calculated UV spectral data of product **3a** are well consistent with their experimental ones (compound **3a** shows experimental absorption peaks at 271, 320 and 410 nm). Similarly, the absorption peaks of compound **5a** at 270, 320 and 411 nm are consistent with their theoretically calculated absorption peaks at 278, 316 and 410 nm. When **3a** reacts with acetic acid to form hydrogenation product, the lengths of the bond connecting the quinoline ring and pyrazole ring of the product are averaged. In other words, C(10)—C(11) bond is elongated by 0.021 Å, and C(9)—C(10) and C(11)—C(12) bonds are shortened by 0.036 Å and 0.031 Å, respectively. In the meantime, dihedral angle C(11)—C(12)—C(13)—C(18) of the hydrogenation product is 174.75°, larger than that of **3a** (163.25°). This implies that the hydrogenation reaction of compound **3a** in acetic acid expands the delocalization of the conjugated systems thereby tending to average the lengths of related bonds. Furthermore, according to the energy levels in association with homologous frontier orbitals, the energy gap value, ε, between the highest occupied molecular orbital and the lowest unoccupied molecular orbital (HOMO–LUMO) of the hydrogenation product is smaller than that of reactant **3a** (reactant **3a** and its hydrogenation product have ε of 4.218 eV and 3.673 eV, respectively). Similar calculation results are also obtained for compound **5a**. By comprehensively considering the geometric structures and electronic transitions, we can infer that, compared with reactants **3a** and **5a**, the changes in the spectroscopic properties of their hydrogenation products are attributed to enlarged conjugated system with enhanced molecular planarity and decreased energy gap of HOMO–LUMO.

The effect of triethylamine on UV–vis spectra of compounds **3a** and **5a** is shown in Figs. 10 and 11. It can be seen that the absorbance obviously increases and the absorption peak position slightly red-shifts with increasing concentration of triethylamine. This suggests that the alkaline medium may influence the intramolecular charge distribution of compounds **3a** and **5a** thereby affecting their spectral properties. In other words, the alkaline medium may facilitate the formation of new species containing —O^- groups that are combined with —NEt_3 and —OH, thereby changing molecular dipole moment.

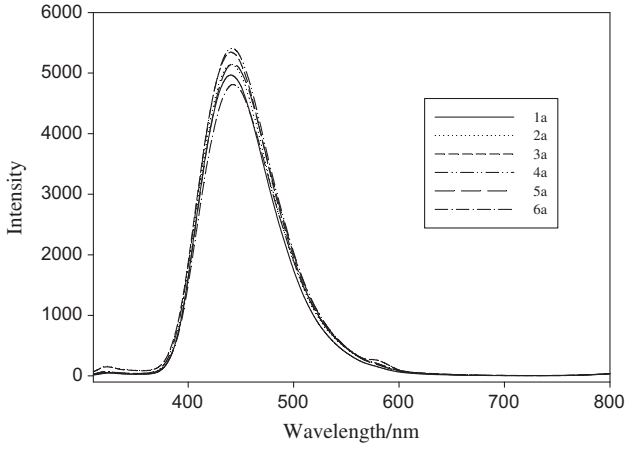

Fig. 5. Fluorescence spectra of compounds **1a**–**6a**.

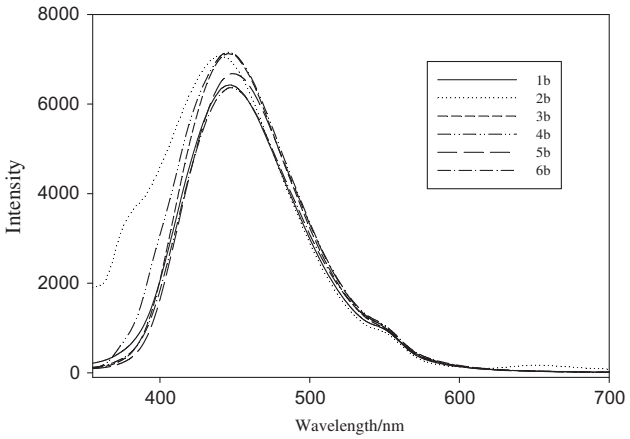

Fig. 6. Fluorescence spectra of compounds **1b**–**6b**.

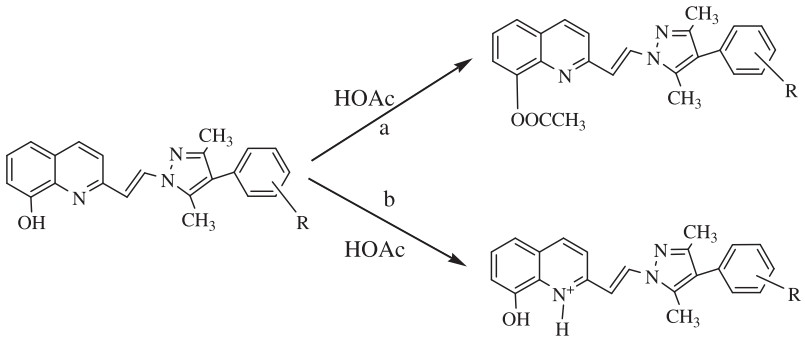

Fig. 7. Possible reaction of hydroxyquinoline compounds with HOAc.

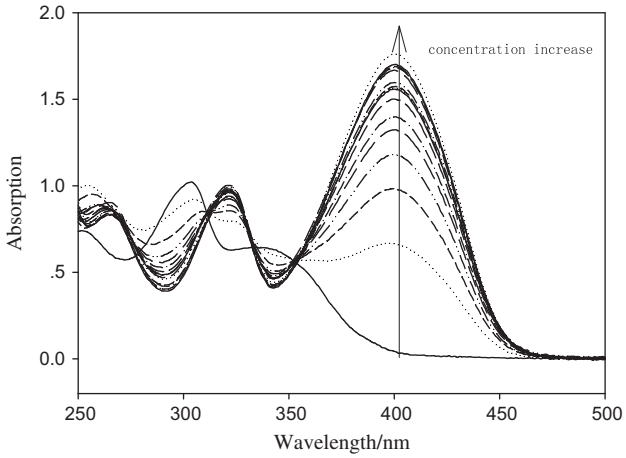

Fig. 8. Influence of acetic acid on UV–vis spectra of **3a**.

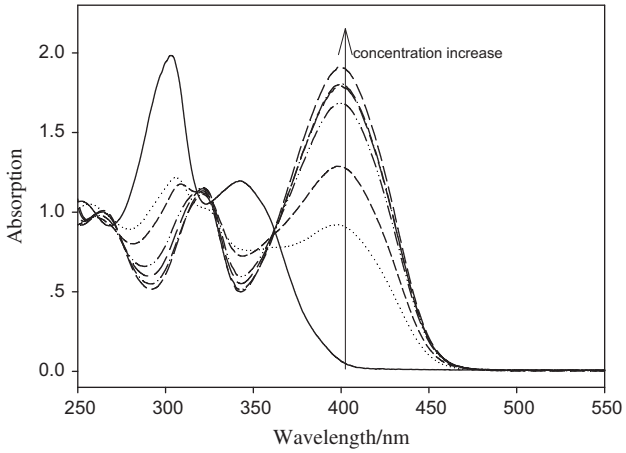

Fig. 9. Influence of acetic acid on UV–vis spectra of **5a**.

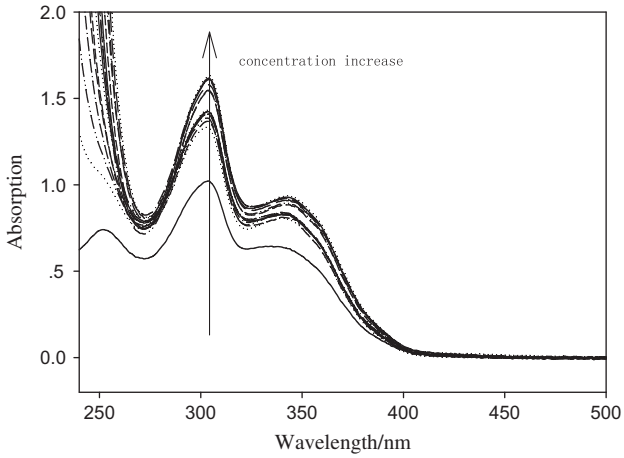

Fig. 10. Influence of triethylamine on UV–vis spectra of **3a**.

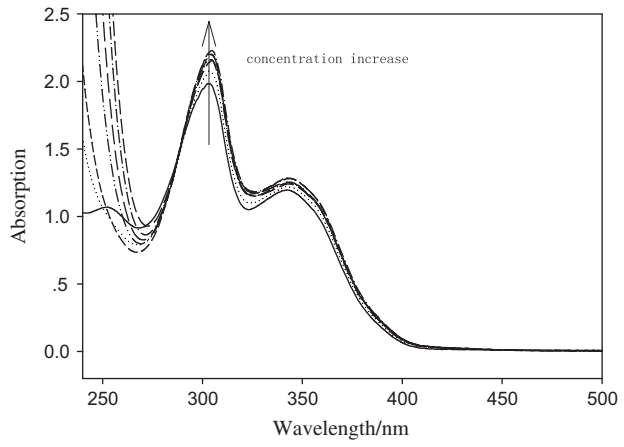

Fig. 11. Influence of triethylamine on UV–vis spectra of 5a.

*Influence of acidity or alkalinity of mediums on fluorescence spectra of compounds **3a** and **5a***

The influence of acetic acid on the fluorescence spectra of compounds **3a** and **5a** is shown in Figs. 12 and 13. It can be seen that synthetic products **3a** and **5a** show two new emission peaks at 344 nm and 582 nm after they react with acetic acid. Obviously, the fluorescence intensity of the maximum emission peak at 440 nm obviously decreases and the emission peak position slightly red-shifts with increasing concentration of acetic acid. This implies that the hydrogenation product containing enlarged conjugated system attributed to enhanced molecular planarity and decreased HOMO–LUMO energy gap possesses strong UV–vis absorbance but weak fluorescence emission, which is possibly because the interaction between cationic -NH^+ and anionic —Ac^- leads to fluorescence quenching. The new emission peak at 582 nm further confirms that the hydrogenation product contains enlarged conjugated system and decreased HOMO–LUMO energy gap as compared with compounds **3a** and **5a**.

The effect of triethylamine on the fluorescence spectra of compounds **3a** and **5a** is shown in Figs. s5 and s6. It can be seen that the reaction of **3a** and **5a** with triethylamine leads to a new emission peak at 545 nm, and the fluorescence intensity of the maximum

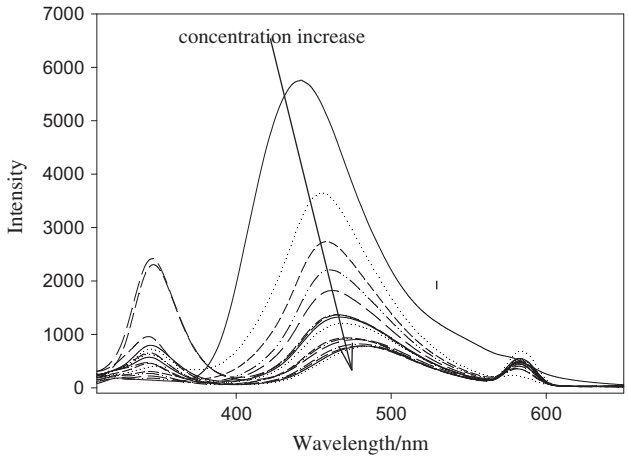

Fig. 12. Effect of acetic acid on fluorescence spectra of **3a**.

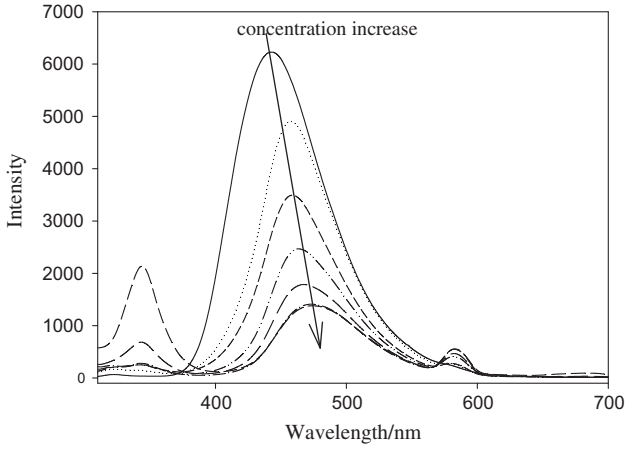

Fig. 13. Effect of acetic acid on fluorescence spectra of **5a**.

Table 1
Inhibition rates of compounds **1b** and **3b** to K562 cell lines.

Compound	K562 (%)	
	10 μmol L^{-1}	30 μmol L^{-1}
Amonafide	18.5	39.0
1b	0	4.5
3b	22.6	15.9

emission peak at 440 nm obviously decreases while the emission peak position slightly red-shifts with increasing concentration of triethylamine. The possible reason is that the interaction of cationic $-^{+}NHEt_3$ and anionic $-O^{-}$ leads to fluorescence quenching of compounds **3a** and **5a** in triethylamine. Namely, newly generated species containing $-O^{-}$ groups contain enlarged conjugated system and enhanced molecular planarity thereby leading to new emission peaks at 545 nm.

In vitro antitumor activity

We predict that the synthetic products have biological activity for the quinoline derivatives and pyrazole derivatives have been widely used in biomedical fields. For this reason, we choose compounds **1b** and **3b** as examples to explore their *in vitro* antitumor activity. Their antiproliferative activity against K562 (human leukemia cell line) was evaluated by *in vitro* MTT assays. Amonafide was tested as a reference compound. The biological results were shown in Table 1. It can be seen from Table 1 that the compounds **1b** and **3b** have showed antiproliferative activity against K562 and can inhibit the growth of K562 cells.

Conclusions

Two series of novel quinoline derivatives containing pyrazole group have been successfully synthesized in high yields with a simple condensation reaction route. The molecular structure of **1a** and **6b** as representative examples were determined by single-crystal X-ray diffraction. The UV–vis absorption spectra and fluorescent spectra of synthetic products have been systematically investigated, and the influence of acetic acid and triethylamine on their spectroscopic properties has been examined with compounds **3a** and **5a** as typical examples. It has been found that synthetic quinoline derivatives containing pyrazole group have good fluorescent properties, and the introduction of acetic acid and triethylamine changes the acidity or alkalinity of medium environment thereby influencing the fluorescent characteristics of synthetic products. Moreover, it is feasible to manipulate the molecular structure and spectroscopic properties of pyrazole and quinoline derivatives by properly adjusting the acidity of medium. This, hopefully, is to help to promote and broaden the application of pyrazole and quinoline derivatives in material science, medicine and ion recognition.

Appendix A. Supplementary material

Supplementary data associated with this article can be found, in the online version, at http://dx.doi.org/10.1016/j.saa.2014.03.018.

References

[1] D. Du, J.X. Fang, Chin. J. Org. Chem. 27 (2007) 1318–1336.
[2] S.J. Kesten, J. Johnson, L.M. Werbel, J. Med. Chem. 30 (1987) 906–911.
[3] K. Mekouar, J.F. Mouscadet, D. Desmaële, F. Subra, H. Leh, D. Savouré, C. Auclair, J. d'Angelo, J. Med. Chem. 41 (1998) 2846–2857.
[4] M. Ouali, C. Laboulais, H. Leh, D. Gill, D. Desmaële, K. Mekouar, F. Zouhiri, J. d'Angelo, C. Auclair, J.F. Mouscadet, M. Le Bret, J. Med. Chem. 43 (2000) 1949–1957.
[5] A.F. Mohammed, F. Alain, P. Eric, M. Jean-François, F. Xavier, H. Reynald, F. Bruno, Bioorg. Med. Chem. Lett. 11 (2003) 5013–5023.
[6] S. Thomas, M. Roger, M. Roland, N. Patrice, R. Michael, K. Zhang, Org. Proc. Res. Dev. 8 (2004) 663–665.
[7] C.W. Tang, S.A. VanSlyke, Appl. Phys. Lett. 51 (1987) 913–915.
[8] E.C. Okafor, B.A. Uzoukwu, Radiochim. Acta 51 (1990) 167–172.
[9] A. Tong, Y. Akama, S. Tanaka, J. Chromatogr. A 478 (1989) 408–414.
[10] K.P. Chirag, C.S. Rami, B. Panigrahi, C.N. Patel, J. Chem. Pharm. Res. 2 (2010) 73–78.
[11] A. Bali, Y. Bansal, M. Sugumaran, J. Singh Saggu, P. Balakumar, G. Kaur, G. Bansal, A. Sharma, M. Singh, Bioorg. Med. Chem. Lett. 15 (2005) 3962–3965.
[12] T.G. Ren, S.Y. Liu, G.H. Li, J.L. Zhang, J. Guo, W.J. Li, L.R. Yang, Spectrochim. Acta A 97 (2012) 167–175.
[13] J. Guo, T.G. Ren, J.L. Zhang, G.H. Li, W.J. Li, L.R. Yang, Spectrochim. Acta A 95 (2012) 135–142.
[14] T.G. Ren, H.B. Cheng, J.L. Zhang, W.J. Li, J. Guo, L.R. Yang, J. Fluoresc. 22 (2012) 201–212.
[15] S.Y. Liu, T.G. Ren, H.B. Cheng, G.H. Li, J. Henan Univ. (Nat. Sci.) 42 (2012) 154–158.
[16] T. Yanai, D.P. Tew, N.C. Handy, Chem. Phys. Lett. 393 (2004) 51–57.
[17] R. Bauernschmitt, R. Ahlrichs, Chem. Phys. Lett. 256 (1996) 454–464.
[18] M.E. Casida, C. Jamorski, K.C. Casida, D.R. Salahub, J. Chem. Phys. 108 (1998) 4439–4450.